Organic & Biomolecular Chemistry

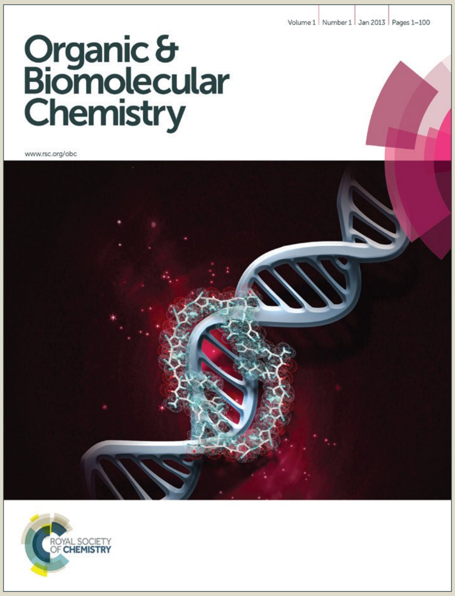

ROYAL SOCIETY OF CHEMISTRY

www.rsc.org/obc

Journal Name

ARTICLE

Readily Prepared Inclusion Forming Chiral Calixsalens

Agnieszka Janiak,*[a,b] Małgorzata Petryk,[b,c] Leonard J. Barbour,*[a] Marcin Kwit*[b,d]

Received 00th January 20xx,
Accepted 00th January 20xx

DOI: 10.1039/x0xx00000x

www.rsc.org/

Calixsalens, chiral triangular hexaimines are readily synthesized by [3+3] cyclocondensation of *trans*-(*R*,*R*)-1,2-diaminocyclohexane with 2-hydroxyisophthalaldehyde derivatives. The usually rigid calixsalen ring is able to invert its conformation as a consequence of steric repulsion between bulky substituents at the C5 positions of the aromatic rings. The steric and electronic nature of the substituents do not affect only the conformation of the macrocycle. Small polar substituents enforce dimeric self-association to form an apohost where each of the monomers simultaneously serves as the host and the guest of its partner. Non-associating calixsalens form assemblies in which two symmetry-related molecules are arranged in head-to-head fashion to form a capsule, or unimolecular cages that are able to entrap solvent molecules in their intrinsic voids.

Condensation of dialdehydes with diamines under thermodynamic conditions produces macrocycles,[1] the overall shape of which depend primarily on the structure of the aldehyde substrate. Chiral macrocycles, which can be synthesized from chiral diamines and/or chiral dialdehydes, are of particular interest.[1,2] Recently, we and others demonstrated that enantiomerically pure *trans*-1,2-diaminocyclohexane (DACH, **1**) readily yields [3+3] products after cyclocondensation with terephthalaldehyde and various unsubstituted and substituted aromatic and aliphatic dialdehydes that also include heteroatoms.[3] After reduction, the imine condensation products yield trianglamines, a new class of flexible chiral polyamine macrocycles with a broad range of applications.[4,5] Introduction of a hydroxyl group to the aldehyde skeleton gives rise to another new class of macrocyclic compounds possessing two types of functionalities, *i.e.* acidic phenol moieties and basic nitrogen atoms.

Hexaimines obtained under template-free thermodynamic conditions from aromatic 2-hydroxy-1,3-dialdehydes and rigid diamines (*e.g.* DACH) assume a vase-like structure and, owing to their likeness to calixarenes, bear the name calixsalens.[6] The upper rim comprises the cyclohexane rings and the halves of phenylene rings containing the hydroxyl and imine substituents. The lower rim is composed of the remaining parts of the phenylene rings having substituents in the *para* positions relative to the hydroxyl groups. The presence of the hydroxyl groups is particularly important owing to their structure-directing and structure-stabilizing characteristics. Calixsalens are particularly attractive as they form multi-metal complexes and exhibit catalytic or fluorescent properties.[6-8]

Here we report the synthesis and structural characterisation of macrocycles **3a**-**3g** from (*R*,*R*)-1,2-diaminocyclohexane **1** and hydroxy-substituted isophthalic aldehydes **2a**-**2g** (Scheme 1). Although some of the macrocycles **3a**-**3g** were previously prepared by us and others,[7-9] there have been no detailed experimental and theoretical studies of their structures, conformations, chiroptical properties in solution, factors that determine their mutual orientation in the solid state, and their inclusion abilities.

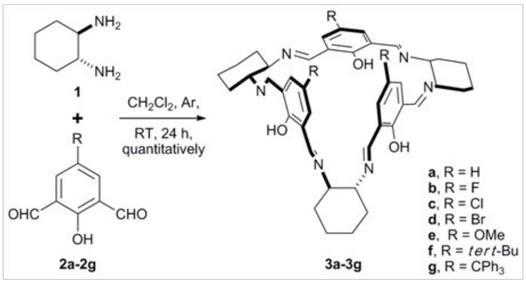

Scheme 1. General procedure for the synthesis of the investigated calixsalens **3a**-**3g**.

Regardless of the size and character of the substituent at the C5 position of the 1,3-dialdehyde skeleton, macrocycles

---

[a] Department of Chemistry and Polymer Science, University of Stellenbosch, Matieland 7602, Stellenbosch, South Africa.
E-mail: agnieszk@amu.edu.pl, ljb@sun.ac.za.
[b] Department of Chemistry, Adam Mickiewicz University, 60-780, Poznan, Poland
E-mail: Marcin.Kwit@amu.edu.pl or mkwit@icho.edu.pl
[c] Wielkopolska Center for Advanced Technologies (WCAT), Umultowska 89C, 61 614 Poznań, Poland
[d] Institute of Organic Chemistry, Polish Academy of Science, Kasprzaka 44/52, 01-224 Warszawa Poland

†Electronic Supplementary Information (ESI) available: details of the synthesis of **3a**-**3g**, along with general experimental protocols and detailed descriptions of the crystallographic procedures and structures. See DOI: 10.1039/x0xx00000x

3a-**3g** can be obtained in quantitative yields by the reaction of equimolar amounts of **1** and **2a**-**2g** under ordinary reaction conditions (Scheme 1). The reaction is apparently driven by the structural predisposition of the intermediate imine products as well as by thermodynamic stability of the macrocycles **3a**-**3g**.

All molecules studied here are homochiral with their stereogenic centers of the *R* absolute configuration. The formal molecular symmetry of each of the molecules **3a**-**3g** is C_3 and the specific structural features are the all-*syn* conformation of the imine bonds and the *s*-*trans* conformation of the diimine fragment.[7b] Although the molecules formally have higher symmetry, they remain asymmetrical in the solid state with the exception of **3f**, which retains its formal symmetry in the crystal. Each of the hydroxyl groups present in the calixsalen acts as an intramolecular hydrogen bond donor to the imine nitrogen atom in the *syn* conformation relating to the hydroxyl group, thus all three hydroxyl H point in the same direction. The presence of intramolecular O-H...N hydrogen bonding introduces a partial rigidity into the macrocyclic skeleton and thereby stabilizes the molecular conformation.

The overall structure of the macrocycle appears to be unaffected by small- and medium-sized substituents attached to the aromatic ring. Taking into account the van der Waals extremities of the hydrogen atoms we estimated the diameters of the upper and lower rims in the macrocycles. The average diameter of the upper rim in calixsalens **3a**-**3f** is 17 Å, whereas the diameter of the lower rim in **3a**-**3d** is *ca* 11 Å and *ca* 12 Å in **3e**-**3f**. However, large substituents such as trityl groups force reversal of the molecular structure through steric repulsion. Thus, in **3g** the triphenylmethyl substituents constitute the upper rim with an estimated diameter of 19 Å, whereas the imine groups with hydroxyl substituents and cyclohexyl rings are situated on the lower rim, the diameter of which is estimated at 16 Å (Fig. 1). Such a structural inversion has not previously been reported for the chiral calixsalen-type macrocycles.

Another structural feature resulting from the substitution pattern in the aromatic part of the molecule seems to be its ability to self-associate in the solid state. Two symmetry independent molecules of **3a**-**3e** form dimers by mutual insertion of one of the phenyl rings of each molecule into the cavity of the other macrocycle. Thus each of the monomers simultaneously serves as the host and the guest for its partner (Fig. 2a). This interdigitating motif is observed *inter alia* in the structures of calix[4]arenes[10] and cyclotriveratrylenes.[11] The two phenyl rings are involved in strong $\pi...\pi$ stacking interactions characterized by relatively short centroid-centroid distances, ranging from 3.417 to 3.740 Å (see parameter *l* in Table 1). The presence of substituents other than hydrogen or fluorine atoms leads to less favourable $\pi...\pi$ stacking interactions. The destabilising effect of the substituent attached to the aromatic ring is clearly seen in the centroid-centroid distances, which increases with variation of the substituent from hydrogen to bromine in the order: H<F<OMe<Cl<Br. The highest possible symmetry of the dimers is C_2, which is never attained in any of the crystals of investigated calixsalens.

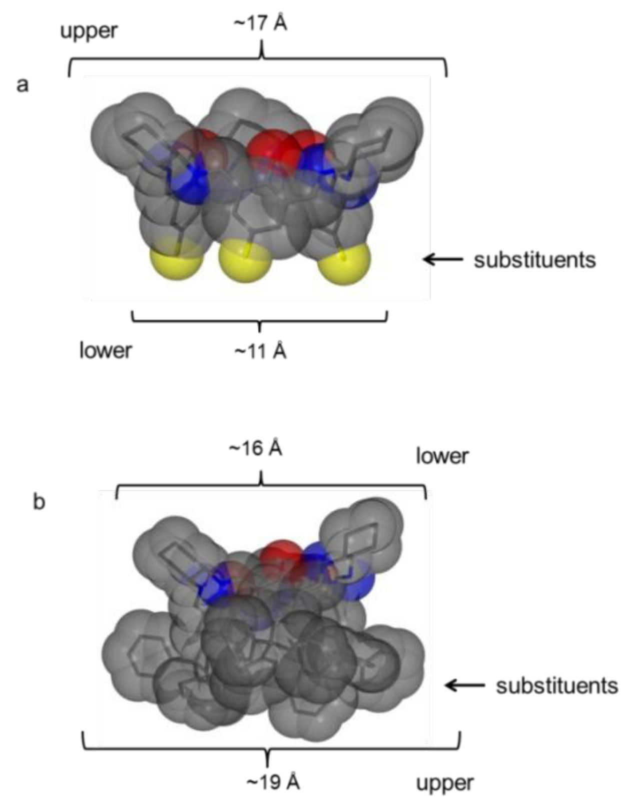

Fig. 1. A van der Waals representation of calixsalen molecules: (a) a representative example of the molecular shape of **3a**-**3f**; (b) the inverted molecular structure of **3g**. Hydrogen atoms are omitted for clarity.

Bulky *tert*-butyl or trityl substituents attached to the aromatic ring prevent interdigitation. These groups form a hydrophobic 'umbrella' over one of the calixsalen rims, thereby limiting access to large moieties. However the second rim still allows the penetration of small guest molecules into its cavity. The overall shape of the molecule does not promote efficient packing in the solid state and **3f** and **3g** thus crystallize as solvated monomers These two calixsalens display slightly different packing modes. Calixsalen **3f** forms a capsule in which two symmetry-related molecules are arranged head-to-head and solvent molecules are entrapped within their cavities (Fig. 2b). In **3g** two symmetry-related host molecules are mutually offset such that that the cyclohexane ring of one molecule is located directly above the entrance to the cavity of the adjacent molecule. In this context the host acts as a molecular organic cage within which one guest molecule is entrapped (Fig. 2c). The remaining guest molecules, if they are in the crystal, surround the external hydrophobic parts of the host molecules (Fig. S21, ESI).

Based on the molecular geometries in the crystals, we optimized the structures of monomers and dimers of **3a**-**3e** using DFT calculations, both in *vacuo* and in dichloromethane solution (see details in ESI). This allowed to estimate interaction energies between respective monomers in the dimer as the difference between dimer energy and the sum of the independently energy minimized monomer energies.

Table 1. Selected geometrical parameters describing π...π interactions[12] within the dimers of calixsalens **3a**-**3e** obtained from the crystals and calculated at the M06L/6-311G(d,p) level in the gas phase (g) as well as in the dichloromethane solution (s)

	l^a [Å]			r^b [Å]		
	X-ray	Calcd (g)	Calcd (s)	X-ray	Calcd (g)	Calcd (s)
3a	3.417(8)	3.396	3.423	0.70(3)	0.87	0.78
3b	3.419(3)	3.333	3.330	0.43(1)	0.51	0.44
3c	3.563(4)	3.446	3.470	1.09(1)	1.14	1.17
3d	3.740(3)	3.460	3.465	1.54(1)	0.77	1.14
3e	3.536(3)	3.435	3.542	1.09(1)	0.78	1.19

[a] The centroid-centroid distance. [b] The offset of interacting rings.

The structures of macrocycles **3a**-**3e** optimized in the gas phase as well as in the presence of the solvent model are generally more compact, *i.e*. the diameter of the lower rim is usually smaller than that observed in the crystal (see Fig S25, ESI).

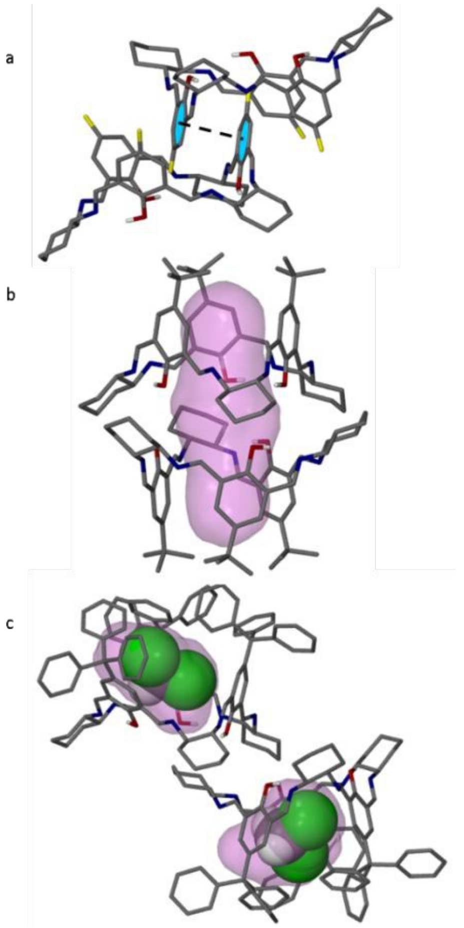

Fig. 2. Types of host packing in calixsalen crystals. (a) Dimeric association of two symmetry-independent molecular hosts as observed in all apohost and/or inclusion crystals of **3a**-**3e**. The phenyl rings involved in the π...π interactions are highlighted in blue. (b) The capsule of **3f**. Due to the high disorder of the solvent molecules, their contributions were removed from the diffraction data using the squeeze.[13] The solvent accessible volume of 58 $Å^3$ is shown as pink Connolly surfaces[14] using a probe radius of 1.45 Å. (c) The molecular cage **3g** with one solvent molecule entrapped in each inner cavity of 35 $Å^3$ (r_{probe}= 1.45 Å). The guest molecules are shown as space-filling models. All H atoms, except for the hydroxyl H atoms and the solvent H atoms, have been omitted for clarity.

Single-point energies calculated for the crystal structures reveal that dimerization energies range from -18.2 to -44.5 kcal mol^{-1} (see Table 2) and may be correlated to the size and electronegativity of the substituent R, as well as formation of a number of weak interactions involving π-electrons, which contribute to the overall dimerization energy. These results are in good agreement with our observations in the solid state (*vide supra*). Moreover, observed X...π or C-H...X contacts in the dimers of **3b**-**3d** (Fig. S24, ESI) are quite repulsive, as reflected in the values of the interaction energies. The values of ΔE decrease from **3a** to **3d**, corresponding to substituents in the order H < F < Cl < Br. Note that the highest interaction energy was obtained for **3e** (R = OMe). In the optimized structures we generally observed a reverse trend to that found for non-optimized structures extracted directly from crystallographic data. Calculated energies suggest that, regardless of the method of calculation, dimerization is strongly preferred both in the gas phase and in solution. Similar association of the calixsalen molecules in the gas phase and in the solution were previously confirmed by other spectroscopic methods, including IM MS, DOSY NMR and OR measurements.[15]

According to the calculations dipole moments in monomers of **3a**-**3e** are polarized along the three-fold symmetry axis of the molecule. In dimers, individual molecules are oriented in order to maximize the stabilizing interaction between two dipoles polarised in opposite directions.

Table 2. Interaction energies (ΔE and ΔΔG, in kcal mol^{-1}) calculated for dimers of calixsalens **3a**-**3e**.

Dimer	Crystal[a]	Gas phase[b]		Dichloromethane[c]	
	ΔE	ΔE	ΔΔG	ΔE	ΔΔG
3a	-24.50	-28.73	-8.21	-40.90	-24.10
3b	-20.29	-32.33	-10.36	-30.17	-5.17
3c	-19.64	-36.30	-18.75	-48.70	-29.91
3d	-18.17	-34.60	-20.51	-51.71	-32.10
3e	-44.55	-40.30	-19.60	-39.07	-20.65

[a] Single-point energy calculated at the M06-2X/6-311G(d,p) level. [b] Optimized at the M06L/6-311G(d,p) level. [c] Optimized at the IEFPCM/M06L/6-311G(d,p) level.

Electronic circular dichroism (ECD) spectra were measured in dichloromethane solution for all of the calixsalens presented here. Additionally, electronic spectra for all stable monomers and dimers were calculated at the IEFPCM/TD-M06-2X/6-311G(d,p) level.[16] As a representative example, experimental and theoretical UV and ECD spectra of **3b** are shown in Fig. 3 (see also Figs. S1-S6 in ESI). In the region of strong absorption the measured UV and CD spectra of **3b** are quite complex. Upon protonation the weak absorption band at ca 350 nm is bathochromically shifted to 450 nm and significantly enhanced. Since there is no change in the structure upon protonation according to the 1H NMR data,[7b] the negative exciton-type couplet corresponding to the long-wavelength UV absorption band corresponds to the negative N-C*-C*-N torsion angle in the diaminocyclohexane moiety. It should be noted that substituents have only a small influence on the band shape and intensity of the electronic spectra of calixsalens **3a**-3**g**.

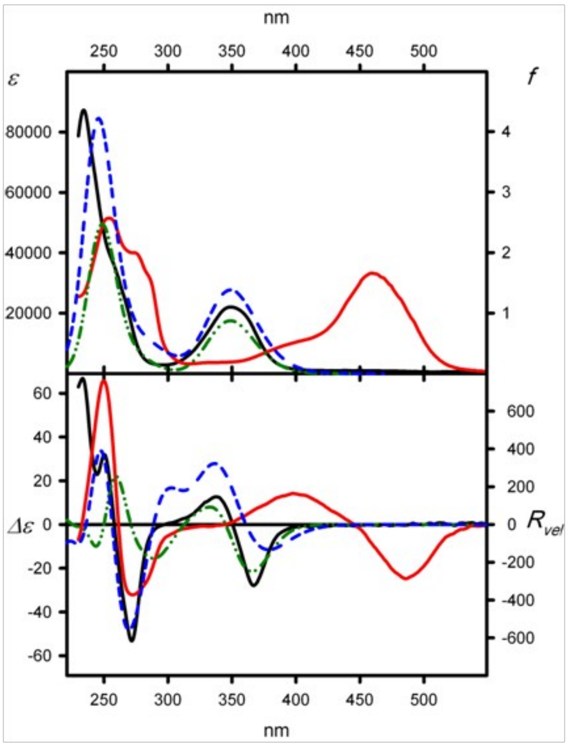

Fig. 3. UV (upper panel) and ECD (lower panel) spectra of macrocycle **3b** measured in dichloromethane (solid black lines), acidified dichloromethane (solid red lines) solutions and calculated at the IEFPCM/TD-M06-2X/6-311G(d,p) level for monomeric (dash-dot-dot dark green lines) and dimeric (dashed blue lines) structures of **3b**. All calculated spectra were wavelength-corrected to match the experimental long-wavelength UV maximum.

Comparison of the experimental UV and ECD spectra of **3b** with those calculated for either the monomer or the dimer shows that better overall agreement is observed for the dimer. Inspection of the spectra reveals that the long-wavelength Cotton effects associated with the UV absorption maximum around 350 nm are a consequence of the intrachromophoric interaction within the individual molecule of **3b**. On the other hand, almost perfect agreement between experimental and calculated spectra for dimeric **3b** in the higher-energy region suggests that these Cotton effects are a superposition of intra- and intermolecular interactions. Similar relationships between experimental and theoretical results were found for the other calixsalens (see ESI for further details).

The change of solvent polarity from a 1:1 mixture of dichloromethane and cyclohexane, through pure dichloromethane and up to a 1:1 mixture of dichloromethane and acetonitrile has a negligible effect on the shape and intensity of the absorption bands.

Conclusions

We have demonstrated a relationship between the size and structure-forming character of the substituent at the C5 position of the aromatic rings of calixsalens. The presence of a relatively small atom at the C5 position promotes self-association of macrocycles into dimeric units, which are also favored in the gas and solution phases. On the other hand, the presence of a less electronegative atom leads to a decrease in the dimerization energy in the solid state and induces opposite energetic effects estimated by DFT methods both in *vacuo* and with the use of the solvent model. However the presence of larger functional groups such as trityl or *tert*-butyl leads to formation of inclusion complexes with a variety of guest molecules. The steric repulsions between trityl groups invert the conformation of the macrocycle.

Acknowledgements

The authors thank the National Research Foundation of South Africa (AJ, LB) and National Science Center in Poland, grant no UMO-2012/06/A/ST5/00230 (MP, MK), for financial support. All calculations were performed at Poznan Supercomputing and Networking Center (grant no 217).

Notes and references

† CCDC-1422957 (**3a**), 1422958 (**3b**), 1422959 (**3c**), 1422960 (**3d**), 1422961 (**3e**), 1422962 (**3f**), 1422963 ($\mathbf{3f_{sCO2}}$), 1422964 (**3g**) and 1422965 ($\mathbf{3g_{MeCN}}$) contain the supplementary crystallographic data for this paper. These data can be obtained free of charge from The Cambridge Crystallographic Data Centre via www.ccdc.cam.ac.uk/data%5Frequest/cif

1 N. E. Borisova, M. D. Reshetova and Y. A. Ustynyuk, *Chem. Rev*., 2007, **107**, 46.
2 S. Srimurugan, P. Suresh, B. Babu and H. N. Pati, *Mini Rev. Org. Chem*., 2008, **5**, 228.
3 see for example: a) J. Gawronski, H. Kołbon, M. Kwit and A. Katrusiak, *J. Org. Chem*., 2000, **65**, 5768; b) M. Chadim, M. Buděšínský, J. Hodačová, J. Zavada and P. C. Junk, *Tetrahedron: Asymmetry*, 2001, **12**, 127; c) N. Kuhnert and A. M. Lopez-Periago, *Tetrahedron Lett*., 2002, **43**, 3329; d) N. Kuhnert, G. M. Rossignolo and A. M. Lopez-Periago, *Org. Biomol. Chem*., 2003, **1**, 1157; e) N. Kuhnert, A. M. Lopez-Periago and G. M. Rossignolo, *Org. Biomol. Chem*., 2005, **3**, 524; f) N. Kuhnert, C. Straßnig and A. M. Lopez-Periago, *Tetrahedron: Asymmetry*, 2002, **13**, 123; g) N. Kuhnert, N. Burzlaff, C. Patel and A. Lopez-Periago, *Org. Biomol. Chem*., 2005, **3**, 1911; h) M. Kwit, P. Skowronek, H. Kołbon and J. Gawronski, *Chirality*, 2005, **17**, S93; i) J. Gawronski, M. Brzostowska, M. Kwit, A. Plutecka and U. Rychlewska, *J. Org. Chem*., 2005, **70**, 10147; j) M. Kwit, A. Plutecka, U. Rychlewska, J. Gawronski, A. F. Khlebnikov, S. I. Kozhushkov, K. Rauch and A. de Meijere, *Chem. Eur. J*., 2007, **13**, 8688.
4 J. Gawronski, K. Gawronska, J. Grajewski, M. Kwit, A. Plutecka and U. Rychlewska, *Chem. Eur. J*., 2006, **12**, 1807.
5 see for example: a) J. Gao and A. E. Martell, *Org. Biomol. Chem*., 2003, **1**, 2801; b) K. Tanaka and S. Hachiken, *Tetrahedron Lett*., 2008, **49**, 2533; c) J. Gajewy, M. Kwit and J. Gawronski, *Adv. Synth. Catal*., 2009, **351**, 1055; d) D. Savoia, A. Gualandi and H. Stoeckli-Evans, *Org. Biomol. Chem.*, 2010, **8**, 3992; e) A. Gualandi, L. Cerisoli, H. Stoeckli-Evans and D. Savoia, *J. Org. Chem*., 2011, **76**, 3399; f) J. Gajewy, J. Gawronski and M. Kwit, *Org. Biomol. Chem*., 2011, **9**, 3863; g) K. Tanaka, A. Asakura, T. Muraoka; P. Kalicki and Z. Urbanczyk-Lipkowska, *New. J. Chem*., 2013, **37**, 2851.
6 a) Z. Li and C. Jablonski, *Chem. Commun*., 1999, 1531; b) Z. Li and C. Jablonski, *Inorg. Chem*. 2000, **39**, 2456.

7 a) S. R. Korupoju and P. S. Zacharias, *Chem. Commun*. 1998, **12**, 1267; b) M. Kwit and J. Gawronski, *Tetrahedron: Asymmetry*, 2003, **14**, 1303.

8 a) K. Tanaka, R. Shimoura and M. R. Caira, *Tetrahedron Lett*., 2010, **51**, 449; b) K. Tanaka, T. Tsuchitani, N. Fukuda, A. Masumoto and R. Arakawa, *Tetrahedron: Asymmetry*, 2012, **23**, 205; c) Y. Fu, Z. Xing, C. Zhu, H. Yang, W. He, C. Zhu and Y. Cheng, *Tetrahedron Lett*., 2012, **53**, 804.

9 a) J. Gao, R. A. Zingaro, J. H. Reinspies and A. E. Martell, *Org. Lett.*, 2004, **6**, 2453; b) J. Gao, J. H. Reibenspies, R. A. Zingaro, F. R. Woolley, A. E. Martell and A. Clearfield, *Inorg. Chem*., 2005, **44**, 232; c) M. Paluch, J. Lisowski and T. Lis, *Dalton Trans.*, 2006, 381; d) Paluch and J. Lisowski, *J. Alloy. Compd*., 2008, **451**, 443.

10 see for example: a) E. B. Brouwer, K. A. Udachin, G. D. Enright, J. A. Ripmeester, K. J. Ooms and P. A. Halchuk, *ChemComm*., 2001, 565; b) G. Dyker, M. Mastalerz, I. M. Muller, K. Merz and K. Koppe, *Eur. J. Org. Chem*., 2005, 4963.

11 see for example: a) M. Salmon, A. Cabrera, N. Zavala, G. Espinosa-Perez, J. Cardenas, R. Gavino and R. Cruz, *J. Chem. Cryst*., 1995, **25**, 759; b) C. Carruthers, T. K. Ronson, C. J. Sumby, A. Westcott, L. P. Harding, T. J. Prior, P. Rizkallah and M. J. Hardie, *Chem. Eur. J*., 2008, **14**, 10286; c) M. A. Little, T. K. Ronson and M. J. Hardie, *Dalton Trans*., 2011, **40**, 12217.

12 U. Rychlewska, A. Plutecka, M. Hoffmann, P. Skowronek, K. Gawronska and J. Gawronski. *Acta Cryst. B*, 2009, **65**, 86.

13 T. L. Spek, *Acta Cryst. A*, 1990, **46**, 194.

14 M. L. Connolly, *Science*, 1983, **221**, 701.

15 M. Petryk, A. Troć, B. Gierczyk, W. Danikiewicz and M. Kwit, *Chem. Eur. J.*, 2015, **21**, 10318.

16 a) N. Harada and P. Stephens, *Chirality*, 2010, **22**, 229; b) M. Kwit, J. Gawronski, D. R. Boyd, N. D. Sharma and M. Kaik, *Org. Biomol. Chem*., 2010, **8**, 5635.

Journal Name

ARTICLE

TOC

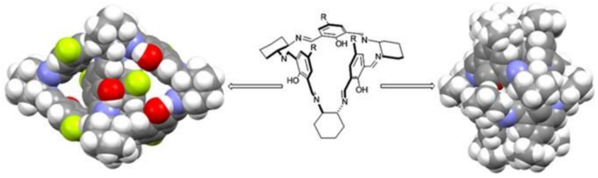

Chiral, rigid vase-like calixsalens show unprecedented substituent-driven self-association and provide supermolecules of contrasting character.